Talanta 99 (2012) 457–463

Contents lists available at SciVerse ScienceDirect

Talanta

journal homepage: www.elsevier.com/locate/talanta

Characterizing natural colloidal/particulate–protein interactions using fluorescence-based techniques and principal component analysis

Ramila H. Peiris, Nicholas Ignagni, Hector Budman, Christine Moresoli, Raymond L. Legge*

Department of Chemical Engineering, University of Waterloo, 200 University Avenue West, Waterloo, ON, Canada N2L 3G1

ARTICLE INFO

Article history:
Received 16 January 2012
Received in revised form
4 June 2012
Accepted 4 June 2012
Available online 9 June 2012

Keywords:
Colloidal/particulate–protein interaction
Fluorescence spectroscopy
Surface plasmon resonance
Principal component analysis

ABSTRACT

Characterization of the interactions between natural colloidal/particulate- and protein-like matter is important for understanding their contribution to different physiochemical phenomena like membrane fouling, adsorption of bacteria onto surfaces and various applications of nanoparticles in nanomedicine and nanotoxicology. Precise interpretation of the extent of such interactions is however hindered due to the limitations of most characterization methods to allow rapid, sensitive and accurate measurements. Here we report on a fluorescence-based excitation–emission matrix (EEM) approach in combination with principal component analysis (PCA) to extract information related to the interaction between natural colloidal/particulate- and protein-like matter. Surface plasmon resonance (SPR) analysis and fiber-optic probe based surface fluorescence measurements were used to confirm that the proposed approach can be used to characterize colloidal/particulate–protein interactions at the physical level. This method has potential to be a fundamental measurement of these interactions with the advantage that it can be performed rapidly and with high sensitivity.

1. Introduction

Characterization of the interaction between protein- and colloidal/particulate-like substances is an area of growing importance for environmental, nanomedical, biotechnological and industrial purposes. These interactions are known to play a pivotal role in a variety of areas such as the formation of protein coronas on nanoparticles [1–4], intracellular uptake and biocatalytic processes that could have biocompatibility issues or adverse biological outcomes [5]. They also play a role in fouling of membranes in many treatment processes including milk production [6] and drinking water treatment [7]. In water purification for example, polysaccharide-like matter contained in the colloidal/particulate fraction of water can interact with protein-like matter and contribute synergistically towards increased membrane fouling [8–10]. These protein–polysaccharide interactions are also of interest due their practical significance in the food industry and applications in biopharmaceuticals as protein carriers [11].

The detection or characterization of interactions at the molecular level involving protein- and colloidal/particulate like species generally require sophisticated techniques such as surface plasmon resonance (SPR), total internal reflection fluorescence microscopy [12], isothermal titration calorimetry (ITC) [1], colloid probe atomic force microscopy (CP-AFM) [13], fluorescence correlation spectroscopy (FCS) [4], scanning electron microscopy (SEM), confocal microscopy and transmission electron microscopy (TEM) [5]. These methods are time consuming, difficult to perform and sometimes have low sensitivity at the very low concentration levels of protein- and colloidal-like matter often found in natural systems. In addition, the use of these techniques for detection and characterization of the protein–colloidal/particle interactions has been limited to model systems. This is due to the challenges in the isolation of protein- and colloidal/particulate-like matter from natural systems. The ability to characterize these interactions in natural systems is a fundamental prerequisite for developing applications that are beneficial for the advancement of nanobiology, nanomedicine, nanotoxicology and membrane-based treatment processes.

This work describes the development of a novel fluorescence excitation–emission matrix (EEM)-based technique that utilizes principal component analysis (PCA) to extract information related to the interactions between colloidal/particulate- and protein-like matter present in natural systems. This approach is suitable for rapid characterization of colloidal/particulate- and protein-like matter with high sensitivity [7,14], eliminates the need for isolation prior to examining their interactions and exploits the intrinsic fluorescence properties of these materials. This has the advantage of avoiding potential sources of measurement error associated with fluorescent labeling and corresponding imaging techniques such as label instability, altered physicochemical properties and photo-bleaching from light/laser exposure [5].

* Corresponding author. Tel.: +1 519 888 4567x33376; fax: +1 519 746 4979.
E-mail address: rllegge@uwaterloo.ca (R.L. Legge).

0039-9140/$ - see front matter © 2012 Elsevier B.V. All rights reserved.
http://dx.doi.org/10.1016/j.talanta.2012.06.010

Mixtures of colloidal/particulate- and protein-like (CPP) matter were extracted using ultrafiltration (UF) from natural river water. Fluorescence EEMs including the light scattering regions of collected spectra for these samples were then analyzed using PCA to extract principal components (PCs) related to colloidal/particulate- and protein-like matter. These PCs were then used for characterization of the protein–colloidal/particle interactions in the extracted CPP samples. The physical interactions between the colloidal/particulate- and protein-like material in CPP extracts were also verified using SPR analyses. This was accomplished by studying the association and disassociation behavior of colloidal/particulate- and protein-like matter to self-assembled monolayers (SAM) prepared by coating 11-mercaptoundecanoic acid (MUA) on gold plated surfaces. 11-MUA forms chemically stable and well-ordered monolayers, generally referred to SAM layers and typically used as a model interface to study the molecular level interactions [15,16]. The presence of colloidal/particulate–protein interactions on this SAM layer was also qualitatively verified by surface fluorescence EEM measurements performed using a fluorescence fiber optic probe, subsequent to the dissociation step of the SPR analysis. The proposed approach should have value in a variety of applications.

2. Material and methods

2.1. Extraction of natural CPP matter

CPP matter samples were extracted from Grand River water (GRW) (Southwestern Ontario, Canada) using a previously described procedure that involves microfiltration and UF stages [7]. Fifteen and 16 different UF experiments were performed using 20 kDa and 60 kDa membranes, respectively, using feed water with seasonal differences of DOC and turbidity to extract natural CPP matter during the period of March 2009–May 2010. A detailed description of this extraction procedure including the quality parameters of GRW used is provided in the Supporting material (SM) section.

2.2. Fluorescence analysis

The fluorescence EEMs of the extracted CPP solutions were recorded using a Varian Cary Eclipse Fluorescence Spectrofluorometer (Palo Alto, CA) by scanning 301 individual emission spectra (300–600 nm) at sequential 10 nm increments of excitation wavelengths between 250 and 380 nm. The procedures used for the fluorescence signal correction and the selection of the spectrofluorometer parameter settings to obtain reproducible fluorescence signals were as previously described [14]. Surface fluorescence measurements were conducted using the same spectrofluorometer and a Varian Cary Remote Read Fiber Optic Probe coupled to the spectrofluorometer with an Eclipse Fiber Optic Coupler. The measurements were conducted on the regions of the MUA coated gold sensor disks where the association/dissociation of the protein and colloidal matter had taken place in the SPR analyzer. This procedure was carried out under controlled humidity conditions. To eliminate background noise, fluorescence spectra of control (MUA coated disks) collected under the same conditions, were subtracted from all spectra. A detailed description of this procedure is provided in the SM section.

2.3. SPR analysis

SPR analyses were performed in triplicate at 25 °C using a cuvette-based AutoLab SPRINGLE (Echo Chemie BV, The Netherlands) analyzer. The SAM layers required for SPR analysis were generated on gold plated disks following the procedure described in the SM section. To understand the interaction behavior of protein-like matter with the SAM layer and to assess the existence of colloidal/particulate–protein interactions in the extracted CPP samples, α-lactalbumin (AL) (average size ~ 10 nm) was used as a surrogate protein. AL was donated by Davisco Foods International, Inc., (LeSueur, MN; Lot #: JE 007–3–921). The association and disassociation behavior of colloidal/particulate- and protein-like matter were then examined by injecting separate solutions (50 μl) of (i) AL (0.5 mg/ml), (ii) CPP (~0.11 mg/ml; calculated based on a dry weight basis) and (iii) a mixture of AL and CPP, containing the same individual AL and CPP concentrations as in (i) and (ii), on to the SAM layer. To ensure the homogeneity of the CPP solution during the SPR analysis, only the suspended part of CPP was used. These solutions were prepared by dissolving appropriate amounts of AL and/or CPP in 20 mM phosphate buffer (pH 7.4). The pH of these solutions was around 7.5. After each association step, the SAM layer was washed with 500 μl of running buffer (20 mM phosphate buffer, pH 7.4) to facilitate the dissociation of the accumulated material (i.e. to remove any loosely bound material). The resulting SPR kinetic curves were zeroed one second after injection to eliminate bulk solution effects. The absence of SPR responses on an inert surface produced using triethylene glycol monoamine [17] confirmed that the binding curves are related to associations and not due to bulk solution effects.

2.4. Principal component analysis

Fluorescence EEM analyses of the solutions of CPP matter extracted for 20 and 60 kDa UF experiments resulted in 15 and 16 fluorescence EEMs, respectively, with each containing 4214 excitation and emission coordinate points. The fluorescence intensity values corresponding to these excitation–emission coordinate points (spectral variables) of a given EEM were organized in a matrix following the previously described fluorescence EEM data rearrangement procedure [14]. This resulted in a 15×4214 fluorescence data matrix for 20 kDa membranes (X20), and a 16×4214 fluorescence data matrix for 60 kDa membranes (X60) with each row containing fluorescence EEM data points of a given sample. PCA was then performed on X20 and X60 data matrices separately to generate the PCs. PCA extracted statistically considerable new variables referred to as PCs that were uncorrelated, orthogonal and mathematically represented by linear combinations of the original variables in X20 and X60 data matrices. Statistically considerable number of PCs in capturing the underlying features in X60 and X20 data sets was determined by using the leave-one-out cross validation method [18]. All computations were performed using the PLS Toolbox 5.2 (Eigenvector Research, Inc., Manson, WA) within the MATLAB 7.8.0 computational environment (MathWorks, Natick, MA).

2.5. Statistical analysis

Analysis of variance (ANOVA) tests were used for statistical analysis. Normality of the data was confirmed using normal probability plots.

3. Results

3.1. Characterization of the colloidal/particulate and protein-like matter extract

The fluorescence EEM of GRW contained peak-α and shoulder-β at an excitation wavelength (Ex) ~ 320 nm and emission wavelength

(Em)~415 nm and at Ex/Em~270 nm/460 nm, respectively, typical of humic substances (HS)-like matter present in water and consistent with the range reported for HS-like components (Fig. 1a) [19,20]. The presence of HS-like matter in GRW was confirmed by independent liquid chromatography-organic carbon detection (LC-OCD) analysis of GRW in the current and previous studies [21,22]. The obvious deviation of the fluorescence EEM contours in the region δ around Ex/Em~280 nm/330 nm results from the presence of a smaller peak that corresponds to protein-like substances in natural water [23,24]. Rayleigh light scattering regions (RS), observed in the fluorescence EEM, contain information related to colloidal/particulate matter present in water [7,14].

Fig. 1b indicates the presence of a predominant amount of colloidal/particulate matter and a comparatively small amount of protein-like matter in the extracted CPP fractions from GRW. HS-like matter in the extracted fractions however appears to be absent (i.e. no fluorescence EEM peaks around regions α and β) indicating the absence or very low levels of HS-like matter. This is consistent with previously reported characteristics of similar extracted fractions from GRW [7]. LC-OCD analysis of the extracted fractions also verified the occurrence of small amounts of protein-like matter (through nitrogen measurements), negligible levels of HS-like matter and predominant levels of organic colloidal matter (through organic carbon measurements). More information about the results of this LC-OCD analysis is provided in SM Fig. S2. Although LC-OCD analysis did not provide information related to the presence of inorganic colloidal and particulate matter, their presence in natural water and hence in the extracted fraction, is expected. Due to these reasons and also the high turbidity levels (28–40 NTU) recorded for CPP extracts during the experimental period, it is reasonable to conclude that the extracted CPP matter contained largely colloidal/particulate-like matter. Due to the methodology employed for extraction of CPP samples [7], the particle size distribution can be expected to vary between the micro ($<200\,\mu m$) and nanoparticle (>10 nm) range. The size distribution of the dissolved portion of the CPP was also determined to be similar to that of protein-, polysaccharide- and organic colloidal-like matter present in natural water as measured through LC-OCD analysis (SM Fig. S2, average size ~20 nm).

3.2. Characterization of colloidal/particulate and protein-like matter using the PCA of fluorescence EEMs

Fluorescence EEM analyses of the CPP extracts, obtained using fifteen 20 kDa and sixteen 60 kDa UF experiments, resulted in two fluorescence data matrices referred hereinafter as X20 and X60 for 20 kDa and 60 kDa UF membranes, respectively. When PCA was performed separately on these matrices, two PCA-based models, each with four statistically considerable PCs, capturing nearly 92% of the total variance present in the raw fluorescence EEM spectral variables (variance captured by each PC > 5%), were generated for X20 and X60. The remaining variance (~8%) was due to the combination of unexplained variance by these PCs and instrument noise (determined to be less than 5% of the intensity readings) in the fluorescence measurements and could be captured by including additional PCs. However, additional PCs were not considered as they were not statistically considerable (less than ~3% variance captured by each additional PC) and not found to be directly related to any organic and colloidal/particulate fraction present in water. To understand the physical significance of each of the PCs generated by this process for X20 and X60 matrices, their corresponding loading plots were examined as previously explained [7]. This process identified that the magnitudes associated with the first three PCs, namely: PC-1, PC-2 and PC-3 were directly related to the amounts of the colloidal/particulate, HS-like and protein-like matter, respectively. Thus their concentrations are directly correlated with the corresponding PC scores (i.e. values of PC). On the other hand, the fourth PC: PC-4, did not show an apparent correlation with any of the major dissolved or colloidal/particulate components mentioned above. A detailed description of this analysis is found in SM.

PCA analysis of fluorescence EEM data resulted in statistically significant PCs that captured systematic trends in the original fluorescence EEM data set. This process also de-convoluted the convoluted information present in the original fluorescence EEM data, in the form of possible residual signals of scattered light that may have propagated into the fluorescence regions. PCs, which were not statistically significant, could theoretically capture some of the artifacts in the original fluorescence signals caused by the propagation of scattered light which are not systematic in the data set (i.e., noise). The statistically insignificant PCs were discarded (i.e., mathematically filtered out) from the analysis. It is noteworthy that a considerable part of the light scattering data is systematically correlated to colloidal/particulate matter and represented by PC1, which is statistically significant.

3.3. Identification of colloidal/particulate–protein interaction using PCs

Since the fluorescence EEM peak-δ is related to the presence of protein or tryptophan-like matter, the fluorescence intensity at peak-δ is expected to have a strong correlation with protein content in the extracted fractions [25]. Also as PC-3 is directly

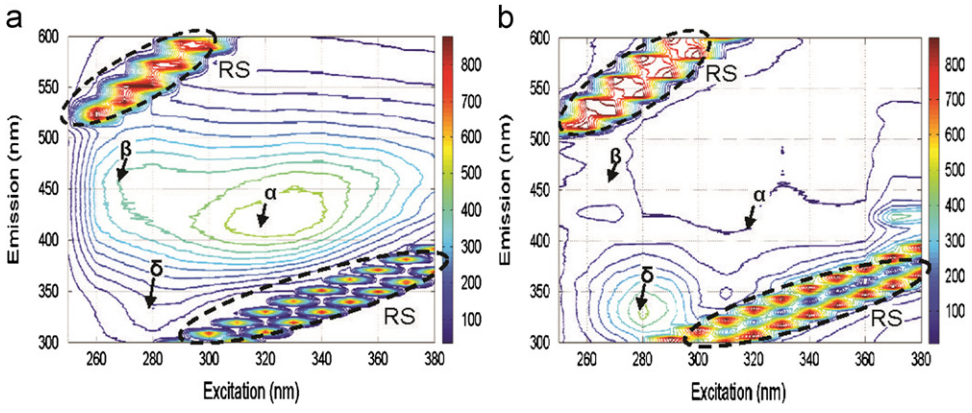

Fig. 1. Typical fluorescence excitation–emission matrices (EEMs) of (a) Grand River water (GRW) and (b) colloidal/particulate and protein-like (CPP) matter extracted from GRW. The intensity scales in arbitrary units (a.u.) are color coded and presented by contours and the scale bars.

correlated with the protein-like content, one would expect a strong correlation between the fluorescence intensities at peak-δ and PC-3 scores. Fig. 2a and b demonstrates fairly strong (R^2=0.78) and moderate (R^2=0.51) correlations between the measured intensities at peak-δ and PC-3 scores for 20 kDa and 60 kDa UF membrane extracted CPP matter, respectively. The general equation of the trend lines that captured these correlations can be described in the form of

$$Intensity = \beta_1 \text{PC-3} + \beta_2 \quad (1)$$

However, when these measured intensity values were corrected by incorporating into the regression model a term of the form of "PC-1 × PC-3" to account for interaction between colloidal/particulate and protein like matter as shown in Eq. (2), the correlations were considerably improved (R^2=0.99 and 0.86 for 20 kDa and 60 kDa UF membrane extracted CPP matter respectively; Fig. 2a and b). In particular, these improvements were significant for measurement points with high deviations (>30 a.u.) from the correlations identified in Eq. (1) (p-value=0.037 (n=7) and 0.038 (n=7) for 20 kDa and 60 kDa UF membrane extracted CPP matter, respectively, as derived from ANOVA). The values of β_i (i=1,2,3..5) for the two data sets of 20 kDa and 60 kDa UF membrane extracted CPP matter are listed in SM Table S1. When the interactions between other combinations of extracted components were considered by incorporating terms of the form of PC-1 × PC-2, PC-2 × PC-3, PC-1 × PC-4, PC−3 × PC-4 or PC-2 × PC-4 instead of the colloidal/particulate–protein interactions, no considerable improvement to the original correlations were observed.

$$Intensity_{-\ corrected} = \beta_3 \text{PC-3} + \beta_4 \text{PC-1} \times \text{PC-3} + \beta_5 \quad (2)$$

Independent measurement points (i.e. validation data points) for CPP extracted from GRW and Burlington Bay (a branch of lake Ontario, Southwestern Ontario, Canada) water (BBW) that were neither used in the PCA-modeling nor in the generation of the trend lines that captured these correlations are also indicated in Fig. 2a–d. Similar to the measurement points, used in the PCA-modeling, the corrected intensities of these independent points also correlated better with their corresponding PC-3 scores, compared to the measured intensity values, indicating the proposed approach is able to capture the effect of the colloidal/particulate–protein interactions on the measured fluorescence intensities. The existence of physical-level interactions in these extracted CPP samples were further verified through SPR analyses as shown in the following section.

Fig. 2c and d illustrates the absolute differences between the measured and corrected fluorescence intensity at peak-δ vs. PC-3 scores for 20 kDa and 60 kDa UF membrane extracted CPP matter, respectively. These differences are correlated with the contribution of colloidal/particulate–protein interactions on the measured fluorescence EEM intensities at peak-δ. The sign of the differences are indicated on each data marker and at this point, it is not clear whether or not the signs are related to the nature of the interactions between colloidal/particulate and protein-like matter; it is hypothesized that the orientation of these interacted species may attribute to this difference in the sign. Testing this

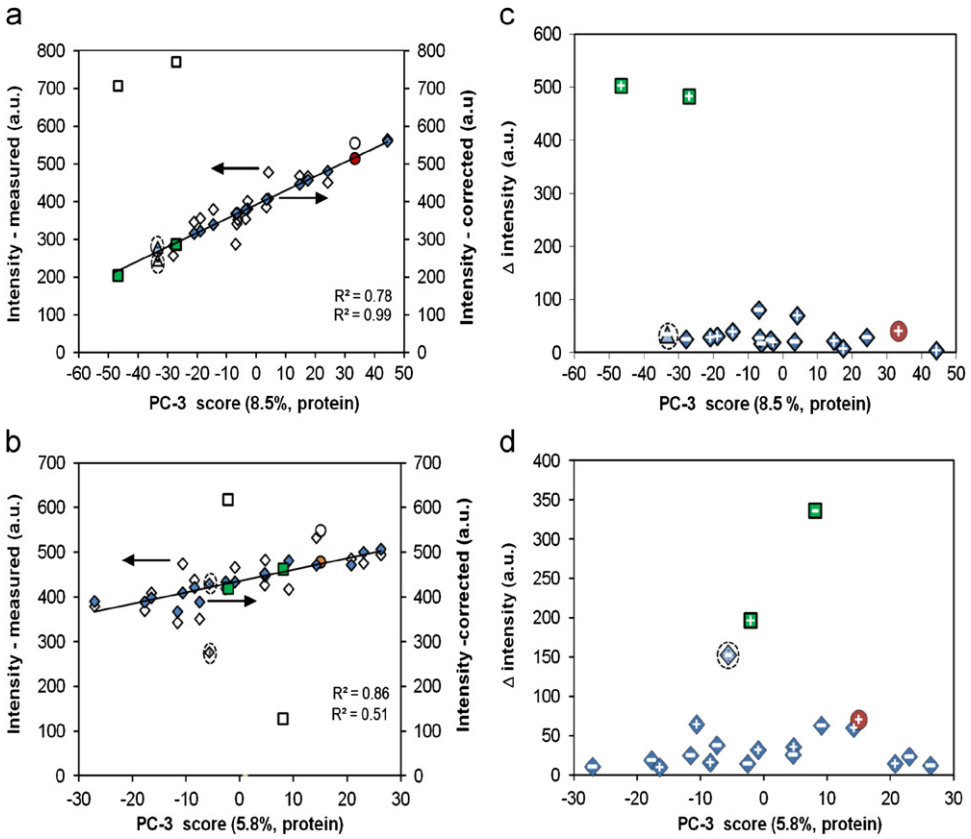

Fig. 2. The plots of measured fluorescence EEM intensities at peak-δ vs. PC-3 scores for (a) 20 kDa and (b) 60 kDa UF membrane extracted colloidal/particulate and protein-like (CPP) matter (◇); improved correlations between corrected fluorescence peak-δ intensities and PC-3 scores (◆). Independent measurement points for extracted CPP from Grand River water (GRW) and Burlington Bay water (BBW) are indicated by "○" and "□", respectively. The corresponding corrected intensity values are identified as " ● " and " ■ ". The plots of absolute differences between the measured and corrected fluorescence peak-δ intensity vs. PC-3 scores for (c) 20 kDa and (d) 60 kDa UF membrane extracted CPP matter are also shown. The sign of the differences are indicated on each data marker. Variance captured by the PC-3 is indicated within the parenthesis.

hypothesis is the current focus of our research. Nevertheless, the absolute values of these differences could serve as a qualitative measurement of the extent and nature of colloidal/particulate–protein interactions present in the samples tested.

To assess the replication and standard deviation of the overall procedure, two new CPP samples, extracted from separate 20 kDa and 60 kDa UF membrane filtration runs, which were not considered in the original PCA model development, were analyzed using the proposed characterization approach (i.e., carrying out the sample through all the steps involved in the proposed approach) five times each ($n=5$). The corresponding measured and corrected average intensity values are indicated with the broken circles in Fig. 2. It should be noted that the error bars of these data points are not clearly visible due to the small standard deviation values. The standard deviation values calculated in this process corresponding to the PC-score for protein-like matter, measured intensity of peak-δ and the corrected intensity of peak-δ were ~2%, 2% and 0.9% respectively of the corresponding average values for the 20 kDa UF membrane extracted CPP matter. The equivalent standard deviation values for the 60 kDa UF membrane extracted CPP matter were ~4%, 3% and 0.05%, respectively. Since the standard deviation values of the proposed approach (i.e., standard deviation of the corrected intensity of peak-δ calculated by incorporating protein–colloidal/particle interactions) are smaller than the differences in the samples (i.e., measured intensity of peak-δ), the reproducibility of the proposed approach can be considered statistically appropriate.

3.4. SPR analysis

SPR response curves provide information related to the association and dissociation of material on the SAM layer of the sensor disk which can be attributed to the molecular- or particle-level physical interaction between the associated materials with this surface. During the association step, materials that are introduced into the system interact with the SAM layer through electrostatic and hydrogen bonding, while the dissociation removes loosely attached material or material where the interactions are weak leaving strongly associated material on the SAM layer [1,26,27].

The SPR sensorgram for the CPP extract shows little or almost no association of material subsequent to the washing (dissociation) step, implemented to remove the loosely associated material, indicating very little or no interaction with the SAM layer (Fig. 3a). In contrast, the sensorgram for AL exhibits an interaction of the AL with the SAM layer as would be expected [28]. When a solution containing both AL and CPP extract with similar concentrations to those for the individual AL and CPP solutions was examined, an intermediate level of interactions as illustrated by the corresponding reduced sensorgram, positioned between the AL and CPP extracts, was observed. In addition, SPR sensograms of the solutions containing the CPP extract and AL shifted towards the AL response curve with a decreasing CPP extract to AL ratio (SM Fig. S4). These results indicate that the CPP extract containing largely colloidal/particulate matter, contributed to reducing the interaction between the AL and SAM layer. This can likely be attributed to inter-molecular or inter-particle physical level interactions between colloidal/particulate content of the CPP and AL that would reduce or mask the sites available for AL molecules to interact with the SAM layer and/or colloidal/particle interactions with the AL that keep the protein–colloidal/particle aggregates suspended and above the penetration depth (PD) of the SPR analyzer (Fig. 3b). Those aggregates that positioned above the SPR signal penetration depth (PD=400 nm for the SPR analyzer used in this study) do not generally contribute to responses related to interactions with the SAM layer [26]. This also explains the absence of an observed interaction between the CPP extract and the SAM layer; colloidal/particulate matter present in the CPP extract would have interacted with comparatively lower protein-like content leaving very limited opportunity for protein-like matter in CPP extract to interact with the SAM layer.

3.5. Fiber optic probe-based fluorescence EEM analysis of the surface of the SAM layer

Surface fluorescence EEMs of the remaining associated CPP extract, AL and the mixture of CPP and AL on the SAM layer were obtained using a fiber optic probe following the SPR dissociation step (Fig. 4a–c). The fluorescence peak near Ex/Em~380 nm/430 nm is due to radiative recombination of holes in the d-band with electrons in the sp-conduction bands of the gold atoms [29] underneath the SAM layer and not related to the associated material. The existence of a clear peak-δ for AL and the mixture of CPP extract and AL signify that the protein remained attached to the SAM layer subsequent to the dissociation step in both cases (Fig. 4b and c), which is consistent with the results of SPR analysis. Also, the absence of a clear peak-δ for CPP extract (Fig. 4a) confirms SPR results, which indicated no considerable

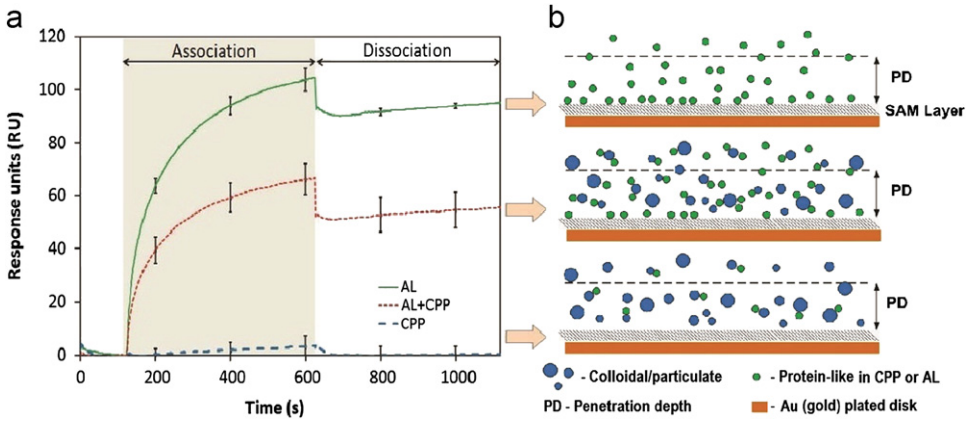

Fig. 3. (a) Surface plasmon resonance (SPR) sensorgrams indicate the association and disassociation behavior of colloidal/particulate and protein-like (CPP) matter, α-lactalbumin (AL) and a mixture of CPP and AL (each with comparable loadings) on the SAM layer of the SPR sensor disk. The error bars represent the standard error ($n=3$) at randomly selected measurement points. The results shown here were obtained using the CPP extract identified as "independent measurement points" in Fig. 2a. (b) A schematic representation of the association between colloidal/particulate and protein-like matter for the three SPR response curves in Fig. 3a. Free protein-like matter showed a higher likelihood of interacting with the SAM layer whereas colloidal/particulate–protein interactions limit the opportunities for protein-SAM layer interactions by reducing or masking the available sites for protein molecules to interact with the SAM layer.

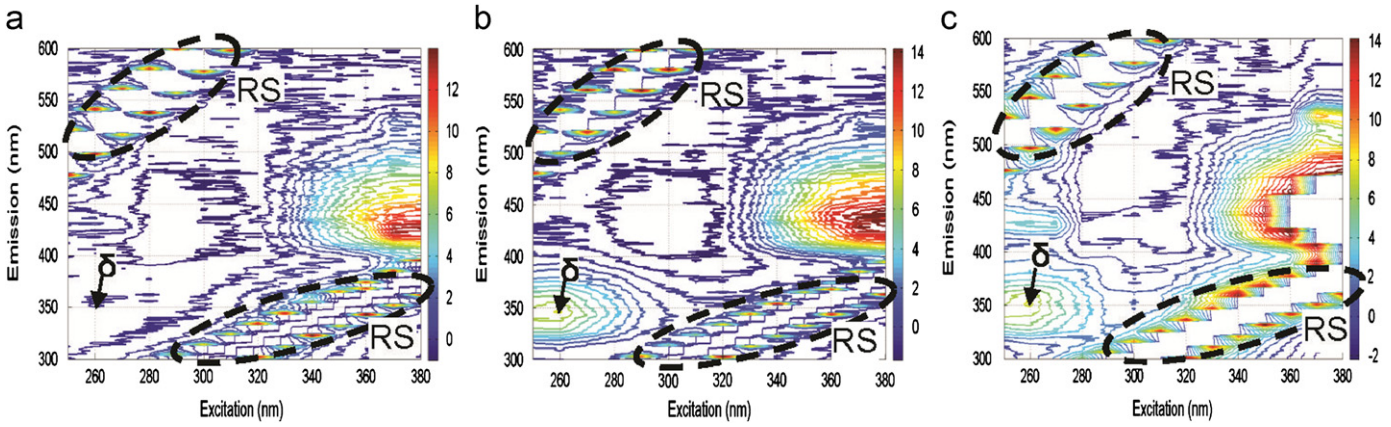

Fig. 4. Fluorescence excitation–emission matrices (EEMs) of the surface of the SPR disk following disassociation step for (a) colloidal/particulate and protein-like (CPP) matter, (b) α-lactalbumin (AL) and (c) a mixture of the CPP matter and AL. The EEMs are limited to an intensity of 14 a.u. (arbitrary units) to allow for a better view of peak-δ.

protein binding to the SAM layer despite the presence of protein-like matter in the CPP extract. The similarity of the magnitudes of the intensity at peak-δ ($\sim$7 a.u.) in both Fig. 4b and c imply that the protein that remained on the SAM layer after the dissociation step was similar for AL and the mixture of CPP extract and AL. On the other hand, the SPR analysis indicated that the amount of AL that interacted directly with the SAM layer was lower for the CPP and AL mixture as compared to the AL solution alone. The increase in the intensity values in the neighborhood of the Rayleigh scattering peaks in Fig. 4c compared to Fig. 4a and b (peaks are not visible as only intensities below 14 a.u. are shown) also indicate an increased level of colloidal/particulate matter on the SAM layer for the mixture of CPP and AL. It is therefore reasonable to conclude that part of AL in the mixture of CPP extract and AL, which did not have direct interaction with the SAM layer would have interacted with colloidal/particulate matter and remained on the SAM layer after the dissociation step. These observations support the above SPR-based assessment of the interaction between colloidal/particulate and protein-like matter that occurred on the surface of the sensor disk.

4. Discussion

The ability to utilize fluorescence EEMs in combination with PCA analysis to capture the physical colloidal/particle–protein interactions in natural systems was demonstrated. This was possible by examining a statistically described interaction term, "PC-1 $\times$ PC-3" that was found to be meaningful for assessing the contribution of colloidal/particle–protein interactions in altering the measured intensities at peak-δ, related to the protein-like matter content in the samples tested. PC-1 and PC-3 scores generated in this approach provided information related to colloidal/particulate and protein-like matter content in the extracted CPP matter, respectively. This novel method of utilizing the PC scores related to colloidal/particulate and protein-like matter to model their interactions was also successfully incorporated in a separate study by the authors to model and forecast membrane fouling [30], demonstrating a possible application of this method in science and engineering disciplines.

The absolute values of the differences between the measured and corrected (Eq. (2)) fluorescence intensity at peak-δ (Fig. 2c and d) are indicative of the level of colloidal/particulate–protein interactions present in the CPP samples extracted from river water over a one year period. Seasonal changes in water over this period would have contributed to very complex and heterogeneous colloidal/particulate and protein mixtures. Despite the complexity of the CPP matter analyzed, the proposed method was validated in terms of its ability to characterize the colloidal/particulate–protein interactions. This was demonstrated with different and independent CPP samples extracted from GRW and BBW that were not used for PCA-modeling (i.e., calibration) (Fig. 2a and b). The level of the interactions captured for CPP samples, extracted from BBW, by this approach were seen to be considerably higher than the samples used in the in the calibration (Fig. 2a–d). These results therefore served for validation of this approach and indicated that the proposed PC-based approach is a fundamental measurement and applicable for characterization of interaction between colloidal/particulate and protein-like mater present in different natural systems. This ability to rapidly characterize the level of colloidal/particulate–protein interactions may have benefits for improving our understanding of a variety of complex phenomena spanning absorption of bacteria onto surfaces [13], biocatalytic processes involving colloidal/nanoparticles [5], biological coating formation on particulate matter [4] and reversible and irreversible membrane fouling [31].

Based on SPR analyses and surface fluorescence EEM measurements, a model was developed that accounts for the interaction between colloidal/particulate and protein-like matter (illustrated in Fig. 3b). According to this model, strong interactions between the SAM layer and protein-like matter are diminished with increasing colloidal/particulate matter content in the solution. High levels of colloidal/particulate content appear to interact readily with the protein in solution and reduce the opportunity for interaction with the protein-SAM layer.

Other techniques for the characterization of colloidal/particulate–protein interactions [1,4,5,12,13] typically have characterization times in the order of hours. Fluorescence EEM analysis of a given sample, in contrast, can be performed within minutes depending on the instrumentation available. Once the fluorescence EEM data has been acquired, the pretreatment of data and subsequent PCA analysis can be performed in less than 10 min, if performed manually. However, if the data pre-treatment and PCA analysis is automated the overall analysis would likely take less than 10 min and as a result the method is considered a rapid characterization technique and of value in adding to the suite of techniques available for characterization of colloidal/particulate–protein interactions.

5. Conclusions

This study proposes a novel fluorescence-based technique to mathematically evaluate the extent of the interaction between

colloidal/particulate and protein-like matter. This was accomplished by the PCA of fluorescence EEM measurements obtained for colloidal/particulate and protein-like mixture samples that were extracted from the natural river water. The proposed approach was also validated using different and independent samples that were not used in the development of this technique. SPR and fiber-optic probe based surface fluorescence measurements corroborate the application of this approach for characterizing colloidal/particulate–protein interactions at the physical level. This technique could serve as a rapid, sensitive and fundamental measurement for evaluating the colloidal/particulate–protein interactions and could be beneficial for a variety of applications including drug delivery systems, water treatment and membrane-based treatment processes.

Acknowledgments

The authors acknowledge funding from the Canadian Water Network and the Natural Sciences and Engineering Research Council of Canada (NSERC).

Appendix A. Supporting information

Supplementary data associated with this article can be found in the online version at http://dx.doi.org/10.1016/j.talanta.2012.06.010.

References

[1] T. Cedervall, I. Lynch, S. Lindman, T. Berggård, E. Thulin, H. Nilsson, K.A. Dawson, S. Linse, Proc. Natl. Acad. Sci. USA 104 (2007) 2050–2055.
[2] M. Lundqvist, J. Stigler, G. Elia, I. Lynch, T. Cedervall, K.A. Dawson, Proc. Natl. Acad. Sci. USA 105 (2008) 14265–14270.
[3] I. Lynch, K.A. Dawson, Nano Today 3 (2008) 40–47.
[4] C. Röcker, M. Pötzl, F. Zhang, W.J. Parak, G.U. Nienhaus, Nature Nanotechnol. 4 (2009) 577–580.
[5] A.E. Nel, L. Madler, D. Velegol, T. Xia, E.M.V. Hoek, P. Somasundaran, F. Klaessig, V. Castranova, M. Thompson, Nat. Mater. 8 (2009) 543–557.
[6] W. Kuhnl, A. Piry, V. Kaufmann, T. Grein, S. Ripperger, U. Kulozik, J. Membr. Sci. 352 (2010) 107–115.
[7] R.H. Peiris, H. Budman, C. Moresoli, R.L. Legge, J. Membr. Sci. 357 (2010) 62–72.
[8] N. Lee, G. Amy, J. Croue, Water Res. 40 (2006) 2357–2368.
[9] D. Jermann, W. Pronk, R. Kagi, M. Halbeisen, M. Boller, Water Res. 42 (2008) 3870–3878.
[10] H. Susanto, H. Arafat, E.M.L. Janssen, M. Ulbricht, Separ. Purif. Technol. 63 (2008) 558–565.
[11] Y. Zhao, F. Li, M.T. Carvajal, M.T. Harris, J. Colloid Interface Sci. 332 (2009) 345–353.
[12] M.M. Baksh, M. Jaros, J.T. Groves, Nature 427 (2004) 139–141.
[13] L. Xu, B.E. Logan, Environ. Sci. Technol. 39 (2005) 3592–3600.
[14] R.H. Peiris, C. Hallé, H. Budman, C. Moresoli, S. Peldszus, P.M. Huck, R.L. Legge, Water Res. 44 (2010) 185–194.
[15] S. Ferretti, S. Paynter, D.A. Russell, K.E. Sapsford, D.J. Richardson, TrAC—Trends Anal. Chem. 19 (2000) 530–540.
[16] J. Stettner, P. Frank, T. Griesser, G. Trimmel, R. Schennach, E. Gilli, A. Winkler, Langmuir 25 (2009) 1427–1433.
[17] F. Frederix, K. Bonroy, G. Reekmans, W. Laureyn, A. Campitelli, M.A. Abramov, W. Dehaen, G.J. Maes, Biochem. Biophys. Meth. 1 (1) (2004) 67–74.
[18] L. Eriksson, E. Johansson, N. Kettaneh-Wold, S. Wold, Umetrics Academy: Umea, Sweden, 2001.
[19] P.G. Coble, S.A. Green, N.V. Blough, R.B. Gagosian, Nature 348 (1990) 432–435.
[20] P.G. Coble, Mar. Chem. 51 (1996) 325–346.
[21] B.R.H. Peiris, C. Hallé, J. Haberkamp, R.L. Legge, S. Peldszus, C. Moresoli, H. Budman, G. Amy, M. Jekel, P.M. Huck, Wat. Sci. Technol.: Water Supply 8 (2008) 459–465.
[22] C. Hallé, P.M. Huck, S. Peldszus, J. Haberkamp, M. Jekel, Environ. Sci. Technol. 43 (2009) 3878–3884.
[23] A. Baker, Environ. Sci. Technol. 35 (2001) 948–953.
[24] N. Her, G. Amy, D. McKnight, J. Sohn, Y. Yoon, Water Res. 37 (2003) 4295–4303.
[25] R.K. Henderson, A. Baker, K.R. Murphy, A. Hambly, R.M. Stuetz, S.J. Khan, Water Res. 43 (2009) 863–881.
[26] E. Stenberg, B. Persson, H. Roos, C. Urbaniczky, J. Colloid Interface Sci. 143 (1991) 513–526.
[27] C.E. Jordan, B.L. Frey, S. Kornguth, R.M. Corn, Langmuir 10 (1994) 3642–3648.
[28] N. Patel, M.C. Davies, M. Hartshorne, R.J. Heaton, C.J. Roberts, S.J.B. Tendler, P.M. Williams, Langmuir 13 (1997) 6485–6490.
[29] A.K. Singh, A.K. Rai, D. Bicanic, Instrum. Sci. Technol. 37 (2009) 50–60.
[30] R.H. Peiris, H. Budman, C. Moresoli, R.L. Legge, AIChE J. 58 (2012) 1475–1486.
[31] M.A. Shannon, P.W. Bonn, M. Elimelech, J.G. Georgiadis, B.J. Marinas, A.M. Mayes, Nature 452 (2008) 301–310.